Amino Acid as a Novel Wettability Modifier for Enhanced Waterflooding in Carbonate Reservoirs

Ricardo A. Lara Orozco, Gayan A. Abeykoon, Mingyuan Wang, Francisco J. Argüelles-Vivas, Ryosuke Okuno, and **Larry W. Lake,** University of Texas at Austin, and **Subhash C. Ayirala** and **Abdulkareem M. AlSofi,** Saudi Aramco

Summary

Reservoir wettability plays an important role in waterflooding, especially in fractured carbonate reservoirs since oil recovery from the rock matrix is inefficient because of their mixed wettability. This paper presents the first investigation of amino acids as wettability modifiers that increase waterflooding oil recovery in carbonate reservoirs.

All experiments used a heavy-oil sample taken from a carbonate reservoir. Two amino acids were tested, glycine and β-alanine. Contact angle experiments with oil-aged calcite were conducted at room temperature with deionized (DI) water, and then at 368 K with three saline solutions: 243 571-mg/L salinity formation brine (FB), 68 975-mg/L salinity injection brine 1 (IB1), and 6898-mg/L salinity injection brine 2 (IB2). IB2 was made by dilution of IB1.

The contact angle experiment with 5-wt% glycine solution in FB (FB-Gly5) resulted in an average contact angle of 50°, in comparison to 130° with FB, at 368 K. Some of the oil droplets were completely detached from the calcite surface within a few days. In contrast, the β-alanine solutions were not effective in wettability alteration of oil-aged calcite with the brines tested at 368 K.

Glycine was further studied in spontaneous and forced imbibition experiments with oil-aged Indiana limestone cores at 368 K using IB2 and three solutions of 5 wt% glycine in FB, IB1, and IB2 (FB-Gly5, IB1-Gly5, and IB2-Gly5). The oil recovery factors from the imbibition experiments gave the Amott index to water as follows: 0.65 for FB-Gly5, 0.59 for IB1-Gly5, 0.61 for IB2-Gly5, and 0.33 for IB2. This indicates a clear, positive impact of glycine on wettability alteration of the Indiana limestone cores tested.

Two possible mechanisms were explained for glycine to enhance the spontaneous imbibition in oil-wet carbonate rocks. The primary mechanism is that the glycine solution weakens the interaction between polar oil components and positively charged rock surfaces when the solution pH is between glycine's isoelectric point (pI) and the surface's point of zero charge (pzc). The secondary mechanism is that the addition of glycine tends to decrease the solution pH slightly, which in turn changes the carbonate wettability in brines to a less oil-wet state.

The amino acids tested in this research are nontoxic and commercially available at relatively low cost. The results suggest a new method of enhancing waterflooding, for which the novel mechanism of wettability alteration involves the interplay between amino acid pI, solution's pH, and rock's pzc.

Introduction

The efficiency of waterflooding depends significantly on the rock wettability in fractured carbonate reservoirs, which often are mixed- or oil-wet. Ultimate oil recovery is usually very small since water cannot imbibe spontaneously into the rock matrix. A change of wettability toward a water-wet state would result in a shift of capillary pressure, changing the capillary pressure from a barrier to a driving force. Therefore, wettability alteration is important to increasing the oil recovery from oil-wet carbonate reservoirs.

The rock wettability is determined by the interactions among crude oil, brine, and rock minerals. In conventional oil reservoirs, the rock surfaces are initially wet by formation brine before oil migration. After the displacement of formation brine by oil, the brine still wets the rock surfaces as long as the brine film remains stable (Buckley et al. 1989). If the brine film becomes unstable, however, the oil contacts the rock surfaces. Then, surface-active oil components are adsorbed on the surfaces, making them less water-wet or even oil-wet. Hirasaki (1991) described that the reversal of the reservoir wettability from oil-wet to water-wet can be achieved by increasing the stability of the thin brine film and/or removing the adsorbed polar components from the rock surfaces.

Low-salinity waterflooding has been studied widely as a method of altering the reservoir rock wettability for enhanced oil recovery (EOR) in carbonate and sandstone reservoirs. A widely used explanation of low-salinity waterflooding in carbonate reservoirs is that low-salinity water can change the wettability of the carbonate rocks by altering the overall charge of the rock surfaces and expanding the electrical double layer of the oil/brine and brine/rock interface (Al Mahrouqi et al. 2017). Many researchers reported that multivalent ions (Ca^{2+}, CO_3^{2-}, Mg^{2+}, and SO_4^{2-}) are the potential determining ions that govern the overall charge of the carbonate rock surfaces (Mahani et al. 2017).

Among many researchers, Austad's research group has extensively investigated the impact of seawater on the oil recovery from carbonate reservoirs (e.g., Høgnesen et al. 2005; Strand et al. 2006; Zhang et al. 2007). Their spontaneous imbibition experiments with seawater indicated that the presence of sulfate ion was responsible for the wettability alteration by displacing carboxylic acids from carbonate surfaces. They also found that calcium and magnesium ions help the sulfate ions to cause the wettability alteration.

Yousef et al. (2011) evaluated the application of low salinity waterflooding by performing core flooding experiments in carbonate media. Their results showed an increased oil recovery of 18% by the sequential injection of seawater and its dilutions. Alotaibi and Yousef (2017) and Ayirala et al. (2018) studied the impact of individual ions in brine on the wettability alteration of carbonate rocks through surface potential experiments. They showed that sulfate and calcium ions were the major-potential determining ions that changed the wettability of the carbonate rocks by decreasing the surface charge to negative values. In combination with the negatively charged crude oil/brine interface, the negatively charged surfaces increased the stability of the water film that promoted a water-wet state.

Copyright © 2019 Society of Petroleum Engineers

This paper (SPE 195907) was accepted for presentation at the SPE Annual Technical Conference and Exhibition, Calgary, Alberta, Canada, 30 September–2 October 2019, and revised for publication. Original manuscript received for review 17 July 2019. Revised manuscript received for review 31 August 2019. Paper peer approved 8 September 2019.

Calcite dissolution has also been proposed as the mechanism for wettability alteration of carbonate rocks. Dissolution was proposed by Hiorth et al. (2010), who tried to match their aqueous and surface complexation model to the imbibition experimental results from Austad's research group. The change of surface potential could not entirely explain the increase in oil recovery. They concluded that calcite dissolution might be the main mechanism for wettability alteration by removal of adsorbed polar oil components.

Experiments on the effect of low-salinity water on carbonate rocks (Chen et al. 2018) indicated that the expansion of the electrostatic double layer caused a short-term effect (around 15 minutes) on the surface wettability. They showed that the mineral dissolution and precipitation caused some surface roughness slowly (more than 12 hours). This series of events was observed by scanning electron microscope imaging.

The ionic interactions described in the literature for low-salinity waterflooding motivated the current investigation of amino acids for wettability alteration of carbonate rocks. Amino acids are nontoxic and biodegradable compounds with two key functional groups—the carboxyl (–COOH) and amino groups ($–NH_2$)—within the same molecule. If these two functional groups are attached to the same carbon atom, it is called α-amino acids (Tripathy et al. 2018). β-amino acids have an additional methylene group between these two functional groups. The current research is focused on glycine (an α-amino acid), the simplest amino acid, and β-alanine (a β-amino acid). These amino acids were selected because of their low cost and high aqueous solubility. **Fig. 1** shows the structures of glycine and β-alanine.

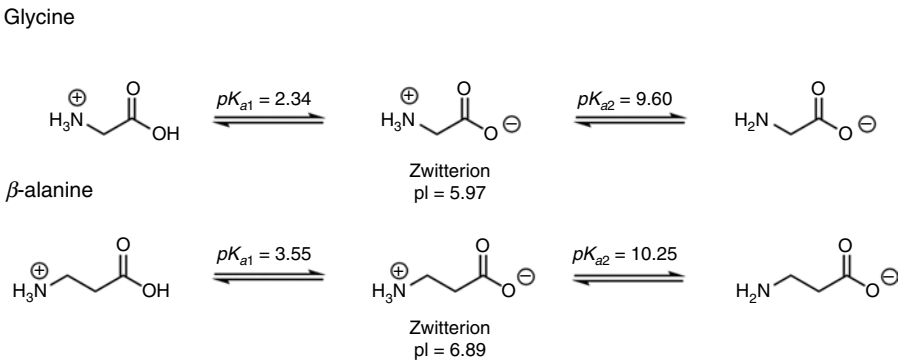

Fig. 1—Chemical structure of the cation, zwitterion (neutral), and anion forms of glycine and β-alanine. The pK_{a1} and pK_{a2} values are the negative base-10 logarithm of the acid dissociation constants of the carboxyl and amino groups, respectively. The pI is the pH at which the amino acid is electrically neutral. Glycine and β-alanine's pI are calculated from the arithmetic average of their corresponding pK_{a1} and pK_{a2} values (Karty 2018).

An important property of amino acids is that their overall charge depends on the solution pH. The pI of the amino acid is the pH value at which the amino acid is electrically neutral in the solution. If the solution pH is higher than the pI, the amino acid is negatively charged overall. Otherwise, the amino acid is overall positively charged. This is caused by deprotonation (release of H^+ proton) of the carboxyl group and ammonium group as the pH increases. The pI of the amino acids with neutral side chains, like glycine and β-alanine, can be calculated directly by taking the arithmetic average of their two pK_a values (pK_a is the negative base-10 logarithm of the acid dissociation constant K_a). The pI values of Glycine and β-alanine are 5.97 and 6.89 at room temperature, respectively (Karty 2018).

The potential application of amino acids as wettability alteration agents comes from the electrostatic interaction between their anionic form with the positively charged calcite surface. Glycine and β-alanine were selected because their pIs reported in the literature are lower than the usual pH values of reservoir and injection brines. Surfactants synthesized from amino acids were studied for chemical EOR applications (Madani et al. 2019) and for other industries (Tripathy et al. 2018). To the best of our knowledge, however, this is the first study of the application of amino acids for EOR.

Materials and Methods

A dead crude oil sample from a carbonate reservoir was used for this research. **Table 1** summarizes properties of the oil sample. The current reservoir pressure and temperature are 26.75 MPa and 372 K, respectively.

Saturates (wt%)	38.7
Aromatics (wt%)	33.9
Resins (wt%)	13.4
Asphaltenes, pentane insoluble (wt%)	14.0
Molecular weight (g/gmol)	314
Total acid number (mg, KOH/g)	0.13
Viscosity at 25°C (mPa·s)	317
Viscosity at 50°C (mPa·s)	62
Viscosity at 80°C (mPa·s)	40

Table 1—SARA analysis, acid number, and viscosity of the crude oil used for contact angle and imbibition experiments. SARA stands for saturations, aromatics, resins, and asphaltenes.

The FB has a salinity of 243 571 mg/L. The injection water for waterflooding is made by mixing two brines, IB1 (68 975 mg/L) and IB2 (6898 mg/L). IB2 is made by a tenfold dilution of IB1 with DI water. In the laboratory experiment, these brines were prepared in a stepwise manner to make the ionic compositions given in **Table 2.** To make one liter of brine, for example, the corresponding amounts of NaCl, $CaCl_2$, and $MgCl_2$ salts were dissolved in 700 cm^3 of DI water, while the Na_2SO_4 and $NaHCO_3$ salts were dissolved in 200 cm^3 of DI water. After stirring for 5 minutes, both solutions were mixed, and an appropriate amount of DI water was added for the total volume of one liter.

Ion	FB	IB1	IB2
Na^+ (mg/L)	70 991	22 928	2293
Ca^{2+} (mg/L)	19 080	2880	288
Mg^{2+} (mg/L)	2561	536	54
Cl^- (mg/L)	150 165	40 500	4050
HCO_3^- (mg/L)	186	366	37
SO_4^{2-} (mg/L)	588	1765	177
Total dissolved solids (mg/L)	243 571	68 975	6898

Table 2—Ionic compositions and salinities of the three brines used in this research.

Glycine and β-alanine samples (Sigma-Aldrich) had a purity greater than 99%. Their molecular structures are presented in Fig. 1. The pI value is 5.97 for glycine and 6.89 for β-alanine at a room temperature of 298 K (Karty 2018). The aqueous stability was confirmed for all amino acid solutions used in this research at their corresponding experimental conditions (temperature, brine composition, and pH).

This paper presents two types of experiments: contact angle and imbibition (spontaneous and forced). They are described in the subsections below.

Contact Angle Experiments. The contact angle experiments were performed by using polished flat pieces of outcrop calcite (Iceland spar). The calcite pieces of approximate dimensions of $5 \times 3 \times 1$ cm^3 were cut from a calcite block and polished using a diamond grinder. The calcite pieces were aged for 1 day in FB (Table 2), and then in the crude oil (Table 1) for at least three weeks at 368 K. This temperature was somewhat less than the reservoir temperature, 372 K, to avoid excessive water evaporation and for safety. After the aging, the calcite pieces were retrieved, and any excess oil was carefully removed from the surface.

The first set of contact angle experiments was focused on the effect of amino acid on the contact angle between oil and water on the oil-aged calcite surface by using DI water with different initial pH values between 3.0 and 10.5, i.e., no brine was used. The solution pH was adjusted for this experiment by adding HCl and NaOH solutions. This fundamental experiment was performed at room temperature since the pIs of the amino acids (5.97 for glycine and 6.89 for β-alanine) and the pzc of the calcite have been reported at room conditions. The reported values of the pzc of the calcite vary from 6.5 to 10.8 depending on the type of calcite, the experimental method, equilibration time, background electrolyte, and CO_2 partial pressure (Al Mahrouqi et al. 2017). For this research, it is reasonable to assume that the calcite pzc is 8.8 as reported by Heberling et al. (2011) on the basis of the zeta potential measurements with Iceland Spar in equilibrium with air (360 ppm CO_2) at 1.0 bar and at room temperature.

The second set of contact angle experiments was concerned with the effect of amino acid on the contact angle for brine compositions at 368 K. Table 2 gave the three brine compositions tested for this contact angle experiment. An appropriate amount of amino acid (glycine or β-alanine) was added to the corresponding brine. All aqueous solutions were placed in an oven at 368 K for at least 1 day to degasify them and avoid the appearance of gas bubbles that may affect the experiment. **Table 3** summarizes the solutions tested in these contact angle experiments.

Solution Name	Solvent	Amino Acid	Concentration (wt%)	Temperature (K)	pH at Room Conditions
DI-Gly5	DI water	Glycine	5	298	3.8, 4.8, 6.9, 7.9, 10.3
DI-Ala5	DI water	β-alanine	5	298	3.7, 4.6, 7.4, 8.3, 10.4
DI water	DI water	–	–	298	4.0, 5.0, 7.5, 8.5, 10.5
FB-Gly5	FB	Glycine	5	368	6.1
FB-Gly1	FB	Glycine	1	368	6.6
FB-Ala5	FB	β-alanine	5	368	7.0
FB-Ala1	FB	β-alanine	1	368	7.0
FB	FB	–	–	368	7.0
IB1	IB1	–	–	368	7.8
IB2	IB2	–	–	368	7.9

Table 3—Summary of the solutions tested in the contact angle experiments. The first three rows correspond to the first set of experiments performed at a room temperature of 298 K, with DI water at different pH values. The solutions presented from row 4 to 7 correspond to the second set of experiments with the brines (Table 2) at 368 K.

Each calcite piece was placed inside a glass chamber with the solution to be tested. Then, five to six oil droplets (depending on the surface area available) were placed on the upper surface of the calcite piece by using a 1.0-cm^3 repeating laboratory dispenser set at a delivery volume of 20 μL. The test chambers were tightly closed. For the second set of experiments, the chambers were placed into the oven at 368 K. For the first experiment, they were kept at room temperature. Pictures of the oil droplets were taken after the initialization and every 24 hours afterward for up to 4 days. The contact angles of both sides of each oil droplet were measured using an onscreen protractor software. An average contact angle from all the droplets was reported for each solution tested.

The contact angle data are subject to heterogeneous surface properties. Obtaining multiple data at different droplet locations helps understand the variability of contact-angle data. Spontaneous/forced imbibition experiments provide more direct information regarding the effect of injection fluid on rock wettability at the core scale.

Spontaneous Imbibition. The spontaneous imbibition experiment was performed to quantify the effect of amino acid on oil recovery solely by water imbibition. This experiment was performed using an Amott cell with a length of 15.24 cm and an internal diameter of 5.08 cm. The neck of the cell is graduated to measure the amount of recovered oil.

Indiana limestone core plugs of 25.4 mm diameter and 127 mm length were used for the spontaneous and forced imbibition experiments in this research. Tagavifar et al. (2018) reported in their X-ray-diffraction analysis that the Indiana limestone mineralogy is predominantly calcite: 0.9 wt% quartz, 97.7 wt% calcite, 0.2 wt% dolomite, 0.6 wt% halite, and 0.6 wt% illite and mica.

The porosity and permeability of each core plug were measured with FB (Table 2) and then saturated with the crude oil (Table 1). The coreflooding system used for saturating the cores consisted of two accumulators for the FB and crude oil, a pump, a Hassler type core-holder, a vacuum pump, a hydraulic manual pump to maintain the overburden pressure, pressure gauges, a differential pressure gauge, and an oven.

The porosity and permeability measurements started by saturating the core plug with FB after evacuation. The effective porosity was determined by subtracting the system's dead volume (3.0 cm^3) from the volume injected. Then, FB was injected at the flow rates of 5, 10, 20, and 30 cm^3/h to determine the permeability from the measured differential pressure. A stable pressure difference was recorded after waiting for 5–30 minutes for each flow rate.

Next, the system was heated to 323 K to decrease the oil viscosity. The oil was injected at a constant flow rate of 2.0 cm^3/h and, after oil breakthrough, the injection rate was gradually increased to 20 cm^3/h to minimize the capillary end effect. The crude oil injection was continued until the water cut became unmeasurable at the terminal injection rate of 20 cm^3/h. The residual water saturation was estimated from the produced brine volume. **Table 4** summarizes the measured porosity, permeability, and residual water saturation for each core plug. The results are similar to those reported in the literature, and indicate a high level of core-scale heterogeneity (Churcher et al. 1991; Ghosh et al. 2018; Wang et al. 2019). Finally, the oil-saturated cores were placed in a container filled with the crude oil for at least three weeks at 368 K.

Core Plug Number	Porosity (v/v)	Brine Permeability (md)	Residual Water Saturation (v/v)
1	0.24	27	0.38
2	0.19	16	0.35
3	0.25	17	0.41
4	0.17	10	0.49

Table 4—Basic petrophysical properties for the Indiana limestone core plugs used in the imbibition experiments.

The four cores prepared (Table 4) were used for imbibition experiments with the following aqueous solutions: IB2, 5.0 wt% glycine in IB1 (IB1-Gly5), 5.0 wt% glycine in IB2 (IB2-Gly5), and 5.0 wt% glycine in FB (FB-Gly5). IB2 was chosen as the base case with no amino acid because a large number of publications on low-salinity waterflooding indicates that IB2 should yield greater oil recovery from a carbonate core than IB1 because its salinity was 10 times smaller than that of IB1 (Myint and Firoozabadi 2015). The aqueous solutions were prepared 1 day before the experiment and placed in an oven at 368 K to minimize the amount of dissolved gas. Excess oil was carefully removed from the core plug surfaces before they were placed inside the imbibition cells. Then, the corresponding solution was carefully poured into the cell. This was done without cooling the solutions and inside a heated oven to minimize any oil recovery caused by thermal expansion of fluids. Oil recovery was periodically monitored during the imbibition experiments at 368 K. **Table 5** summarizes the solutions tested and the corresponding core plugs.

Finally, the glycine concentrations in the aqueous phase in the Amott cell after the spontaneous imbibition experiments were quantified by proton nuclear magnetic resonance (NMR) spectroscopy (^{1}H NMR). The quantification method consisted of obtaining a 3-g sample and adding 100 μL of acetone as an internal standard. Then, the solution was thoroughly mixed before the ^{1}H NMR was taken. The concentration of glycine was calculated on the basis of the amount of acetone added and the ratio of the integration values of the peaks of the glycine molecule's methylene protons (2H) and the acetone molecule's methyl group protons (6H).

Solution Name	Solvent	Amino Acid	Concentration (wt%)	pH at Room Temperature	Core Plug Number
FB-Gly5	FB	Glycine	5	6.1	1
IB1-Gly5	IB1	Glycine	5	6.7	2
IB2-Gly5	IB2	Glycine	5	6.4	3
IB2	IB2	–	–	7.9	4

Table 5—Solutions tested in the spontaneous imbibition experiment at 368 K. The reported pH values correspond to the initial condition before setting up the experiment. The last column indicates the core plugs given in Table 4.

Forced Imbibition. Forced imbibition was performed after the spontaneous imbibition for each core at 368 K. Results were used to calculate the Amott index to water,

$$I_w = \frac{V_{o,\mathrm{SI}}}{V_{o,\mathrm{SI}} + V_{o,\mathrm{FI}}}, \quad \ldots\ldots (1)$$

where $V_{o,\mathrm{SI}}$ and $V_{o,\mathrm{FI}}$ are the volume of oil recovered by the spontaneous and forced imbibition, respectively. The forced imbibition was done at a constant flow rate using the experimental setup used for saturating the cores.

The injection rates for all forced imbibition tests were initially set for a capillary number of approximately 2×10^{-5}. The capillary number, N_{vc}, is

$$N_{\mathrm{vc}} = \frac{v\mu_w}{k^{\circ}_{\mathrm{rw}}\sigma\cos\theta}, \quad \ldots\ldots (2)$$

where v is the interstitial velocity, μ_w is the viscosity of water, k°_{rw} is the endpoint relative permeability for water, σ is the oil/water interfacial tension (IFT), and θ is the oil/water contact angle. It was assumed that $k^{\circ}_{\mathrm{rw}}\sigma\cos\theta = 1\,\mathrm{mN/m}$, a typical value for water-wet media (Lake et al. 2014).

After no oil production was observed for at least two pore volumes (PVs), the injection rate was increased to reduce the capillary end effect by achieving the Rapoport and Leas number (N_{RL}) of approximately 3 cp-cm^2/min. This is a common value used to reduce the capillary end effect in core floods (Lake et al. 2014). N_{RL} (Rapoport and Leas 1953) is defined as

$$N_{\mathrm{RL}} = \mathrm{Lu}\mu \quad \ldots\ldots (3)$$

where u is the superficial velocity in cm/min, L is the core length in cm, and μ is the injected fluid viscosity in cp. **Table 6** summarizes the initial low injection rate and high injection rate, along with their corresponding capillary number, N_{vc}, and the Rapoport and Leas number, N_{RL}.

	Low Injection Rate			High Injection Rate		
Solution	u (ft/D)	N_{RL} (cp-cm^2/min)	N_{vc}	u (ft/D)	N_{RL} (cp-cm^2/min)	N_{vc}
FB-Gly5	4.6	0.37	2.0×10^{-5}	37.1	3.0	1.6×10^{-4}
IB1-Gly5	3.6	0.29	2.0×10^{-5}	37.1	3.0	2.3×10^{-4}
IB2-Gly5	4.8	0.39	2.0×10^{-5}	37.1	3.0	1.6×10^{-4}
IB2	3.3	0.27	2.0×10^{-5}	37.1	3.0	2.0×10^{-4}

Table 6—Superficial velocities, Rapoport and Leas numbers, and capillary numbers for the low and high injection rate used in the forced imbibition experiments.

Experimental Results

This section presents the results of the contact angle and imbibition experiments. There are two sets of contact angle experiments: one with DI water with/without amino acid at a variety of initial pH conditions at room temperature, and the other with three brines at 368 K. Results of imbibition experiments are presented and discussed after the two subsections on the contact angle experiments.

Contact Angle Experiment #1. Fig. 1 showed that the overall charge of amino acid solution depends on how close the solution pH is to the amino acid pI. Glycine, for example, exhibits an overall negative charge if pH > 5.97. Given the calcite pzc of approximately 8.8 at the experiment conditions (Heberling et al. 2011), glycine is expected to enhance wettability alteration when the solution pH is between glycine pI (5.97) and calcite pzc (8.8). The purpose of this first set of experiments was to investigate the interplay among amino acid pI, calcite pzc, and solution pH.

Figs. 2 through 4 show pictures taken right after the initialization and at Day 3 for DI water, 5 wt% glycine in DI water (DI-Gly5), and 5 wt% β-alanine in DI water (DI-Ala5), respectively. As described previously, this experiment was performed at room temperature. **Fig. 5** shows the measured contact angles on Day 3. Note that the horizontal axis in this figure indicates the initial pH values when the experiment was setup. The dissolution of calcite by low pH solutions increased their pH. **Table 7** summarizes the pH values before the experiment and after 15 days. The changes in pH indicate that the calcite dissolution was significant for the experiments with the two lowest pH values (3.8 and 4.8 for DI-Gly5 and 3.7 and 4.6 for DI-Ala5).

The DI-water case resulted in a nonmonotonic trend of average contact angle with respect to the pH. That is, the average contact angle increased from approximately 100 to 150° with decreasing pH from 10.5 to 5.0. This is in line with the reported behavior of the zeta potential of calcite in DI water observed by Mahani et al. (2017) and the relation between the surface charge and wettability presented by Hirasaki (1991). That is, as the pH of the DI water is decreased, the calcite surface becomes more positively charged and, therefore, more oil-wet.

A dramatic reduction in contact angle was observed from 150 to 90° when the pH was reduced from 5.0 to 4.0. This is attributed to the dissolution of calcite, which causes the polar components absorbed on the surface to be released and alters the wettability to less oil-wet (Chen et al. 2018). The calcite dissolution with this low-pH solution was expected because decreasing the solution pH below 5.5 significantly increases the calcite dissolution rate (Brantley et al. 2007).

The glycine case resulted in systematically lower contact angles in comparison to the DI-water case. The monotonic reduction of average contact angle with decreasing pH made the contact angle reduction by glycine more pronounced between 5.0 and 9.0 in the initial pH. Note that this pH range reasonably matches the pI of glycine and the pzc of calcite, as explained previously. For the initial pH of 3.8, the wettability alteration occurred by at least two mechanisms: calcite dissolution and glycine adsorption.

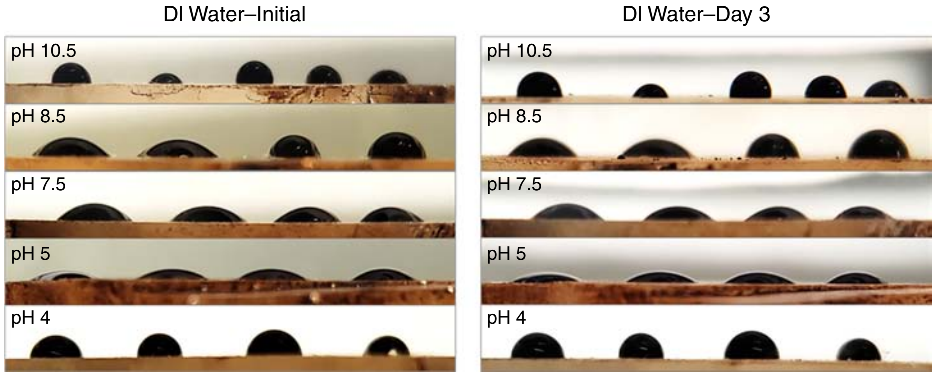

Fig. 2—Initial and final contact angles in the experiment with DI water at different solution pHs.

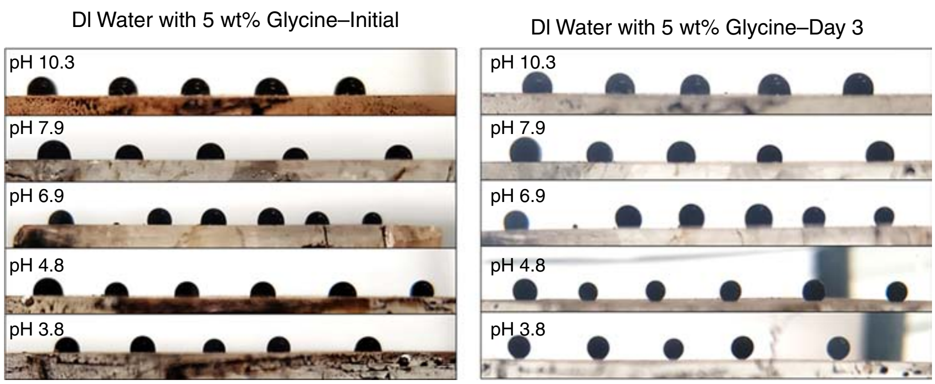

Fig. 3—Initial and final contact angles for DI-Gly5 at different solution pHs. The oil droplets at a pH of 3.8 detached on the fourth day as a result of the wettability alteration by glycine.

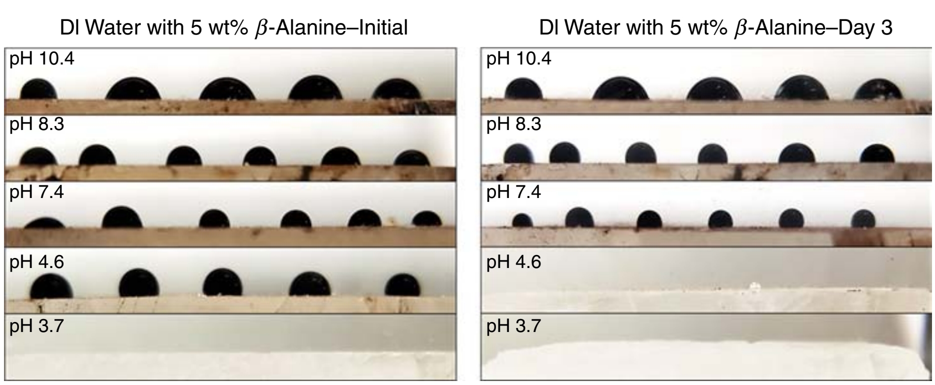

Fig. 4—Initial and final contact angles of DI-Ala5 at different solution pHs. The oil droplets from the solution with a pH of 4.6 detached after the second day. For the solution with a pH of 3.7, it was not possible to place oil droplets on the surface, and bubbles were caused by calcite dissolution.

The β-alanine case gave similar results to the glycine case, but the contact angle values were approximately 20° greater than the glycine case. This is likely because the pI of β-alanine is greater than that of glycine, which makes the pH range between amino acid pI and calcite pzc smaller with β-alanine. It was not possible to obtain data for β-alanine at the initial pH value of 3.7. It appeared that the rapid calcite dissolution made it impossible to place oil droplets on the surface. Oil droplets for the β-alanine case with the initial pH of 4.6 were released from the surface by Day 2.

The interaction of the amino acid with the calcite surface largely explains the observed contact angle reduction when the initial pH was set between the amino acid pI and the calcite pzc. Churchill et al. (2004) investigated the adsorption of amino acids on calcite surfaces at different pH values. They concluded that the charges of the mineral surfaces and amino acids were essential to molecular adsorption, and that a higher degree of adsorption was observed when the amino acid pI was low compared to the calcite pzc.

At initial pH values below 6.0, it is likely that the rapid calcite dissolution (Brantley et al. 2007) was closely coupled with the amino acid interaction with the calcite surface for the observed contact angle reduction. Sjöberg and Rickard (1984) presented that the rate of calcite dissolution at pH values between approximately 4.5 and 5.5 could be approximated by

$$R = k_1(H^+)^{0.90}, \quad (4)$$

where R is the rate of dissolution in mmol/cm^2·s, $[H^+]$ is the activity of hydrogen ion, and k_1 is the rate constant that corresponds to the following calcite dissolution reaction (Plummer et al. 1978):

$$CaCO_3 + H^+ \leftrightharpoons Ca^{2+} + HCO_3^- . \quad (5)$$

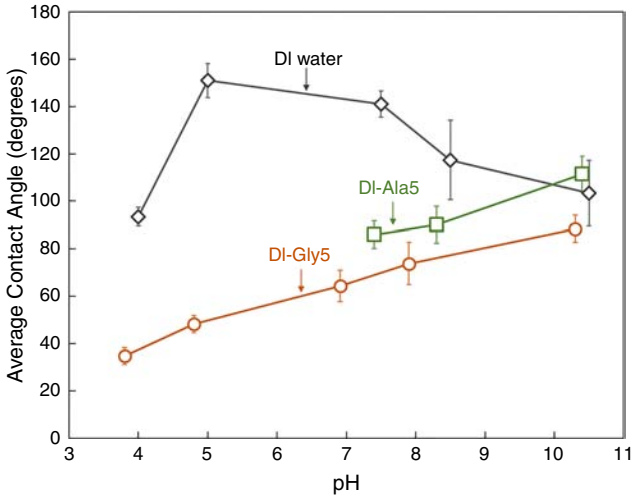

Fig. 5—Average contact angles on Day 3 for DI water, DI-Ala5, and DI-Gly5 solutions. There are no data for DI-Ala5 solution with the initial pH of 3.7 since it was not possible to place oil droplets on the calcite surface. The missing datum for DI-Ala 5 solution with initial pH 4.6 is because of the detachment of oil droplets by Day 2. Initial and final pH values for the solutions are summarized in Table 6.

Solution	Initial pH	Final pH (15 days)
DI-Gly5	3.8	6.1
	4.8	7.2
	6.9	7.5
	7.9	8.3
	10.3	10.6
DI-Ala5	3.7	5.2
	4.6	6.1
	7.4	8.1
	8.3	8.8
	10.4	10.6

Table 7—Initial and final pH values of the solutions in the contact angle experiment presented in Fig. 6. The final pH values were measured after 15 days from the start of the experiment, during which the solution was still in contact with the calcite piece.

Calcite dissolution yields bicarbonate ions, which in turn are converted into carbon dioxide and hydroxyl ions (Langmuir 1997), as given by

$$HCO_3^- \leftrightharpoons CO_2 + OH^-, \quad (6)$$

which increases the solution pH.

The amino acid in the solution tends to suppress the pH increase by the deprotonation of the carboxyl group. In the case of glycine, for example, the reaction given as

$$NH_3^+ - CH_2 - COOH + OH^- \leftrightharpoons NH_3^+ - CH_2 - COO^- + H_2O, \quad (7)$$

tends to prevent the pH increase. This results in a greater amount of calcite dissolution than when the solution does not contain glycine, i.e., the DI-water case.

Contact Angle Experiment #2. As mentioned previously, this second set of contact angle experiments was to quantify the effect of the amino acid on the contact angle with three brine compositions at 368 K. Table 2 presented the compositions of FB, IB1, and IB2. Table 3 presented the solutions tested, FB-Gly5, FB-Gly1, FB-Ala5, and FB-Ala1.

Fig. 6 shows the change in contact angle with FB. The initial average initial contact angle was 114°, which was measured at room temperature. An equilibrium condition at 368 K was reached with an average contact angle of 130°. Results show that the oil-aged calcite surface was oil-wet, and that the FB did not affect the calcite's wettability.

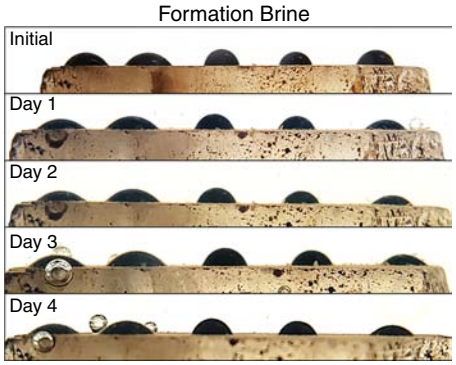

Fig. 6—Contact angle change with time for FB.

Fig. 7 shows the contact angles observed for IB1 and IB2. The initial average contact angle was 100° and 103° for IB1 and IB2, respectively. For IB1, the average contact angle gradually increased to 129°. The average contact angle for IB2 increased up to 108° at Day 2, but then decreased to 102°. **Fig. 8** shows the measured contact angle for IB1, IB2, and FB. A systematic reduction in the contact angle (more water-wet) was observed with decreasing salinity as expected from many studies in the area of low-salinity waterflooding.

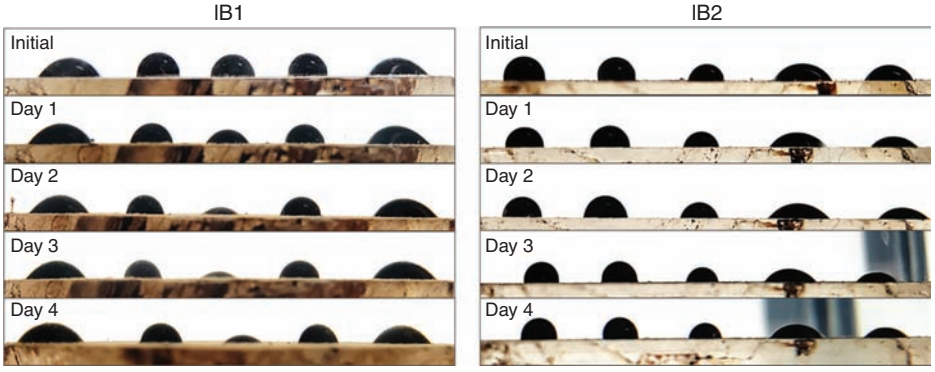

Fig. 7—Contact angle change with time for IB1 and IB2.

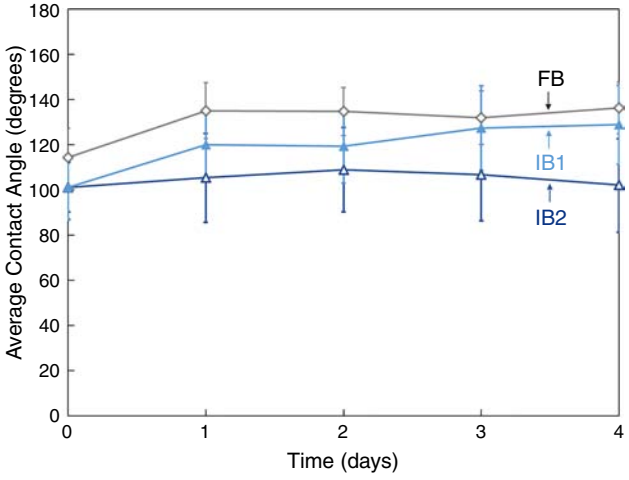

Fig. 8—Contact angle measurements for formation and IBs at 368 K.

Fig. 9 shows the results for FB-Gly1 and FB-Gly5. The initial average contact angle for FB-Gly1 solution was 140°, and it gradually decreased to 134°. The initial average contact angle with FB-Gly5 solution was 98°, and it dramatically decreased to 50°, yielding the calcite surface strongly water-wet. Some of the droplets were detached from the calcite surface as shown in Fig. 9. The measured contact angles of FB-Gly5 and FB-Gly1 are compared to FB in **Fig. 10.**

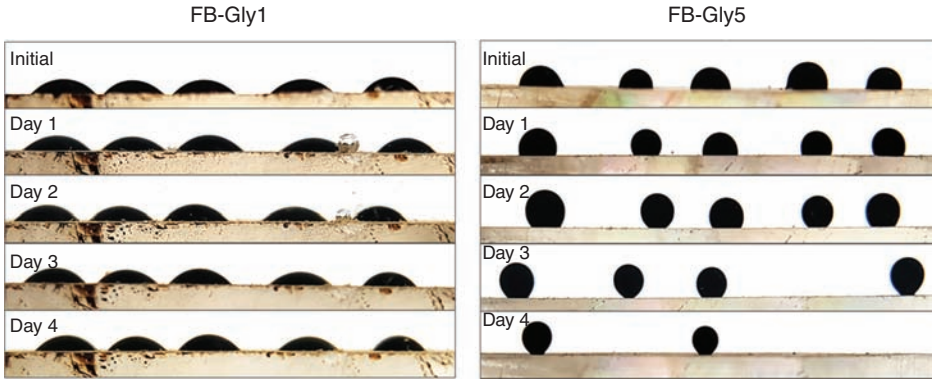

Fig. 9—Contact angle change with time of FB with 1 wt% (FB-Gly1) and 5 wt% glycine (FB-Gly5). For FB-Gly5 solution, oil droplets started to detach on the third day when the buoyancy force is greater than the adhesion force.

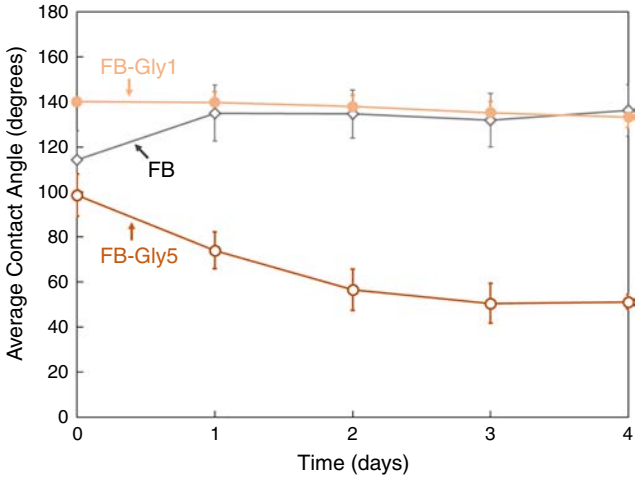

Fig. 10—Contact angle measurements for glycine in FB solutions at 368 K.

Fig. 11 shows the results of FB-Ala1 and FB-Ala5 solutions. The initial average contact angles for FB-Ala1 and FB-Ala5 solutions were 108 and 136°, respectively. The FB-Ala5 solution yielded a more oil-wet surface with a final average contact angle of 142°, while FB-Ala1 solution final average contact angle was 113°. The measured contact angles of FB-Ala5 and FB-Ala1 are compared to FB in **Fig. 12.**

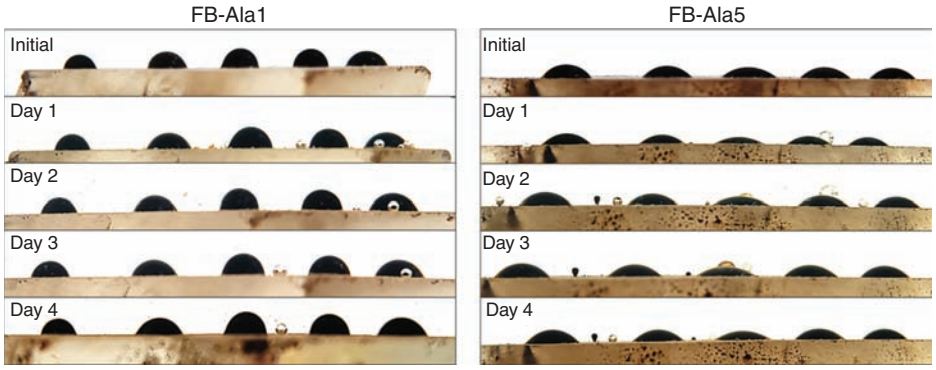

Fig. 11—Crude oil contact angle change with time of FB with 1 wt% (FB-Ala1) and 5 wt% β-alanine (FB-Ala5).

Fig. 13 summarizes the average contact angles for all tested saline solutions. The most important result is the clear reduction in contact angle and the subsequent detachment of oil droplets with FB-Gly5 solution. For the other solutions, the average contact angles were between 100 and 140° (oil-wet), and no clear reduction in contact angle was observed.

Calcite's surface charge depends at least on the brine composition, salinity, and pH. Mahani et al. (2017) measured the zeta potential of the calcite by electrophoresis. Their results show that the calcite was positively charged for a range of pH values between 6 and 10 in an FB with a salinity of 179 855 mg/L. The contact angle results presented above indicate that the calcite piece submerged into the FB was positively charged. This is also implied by the pH values for FB, IB1, and IB2 (7.0–7.9) as given in Table 3.

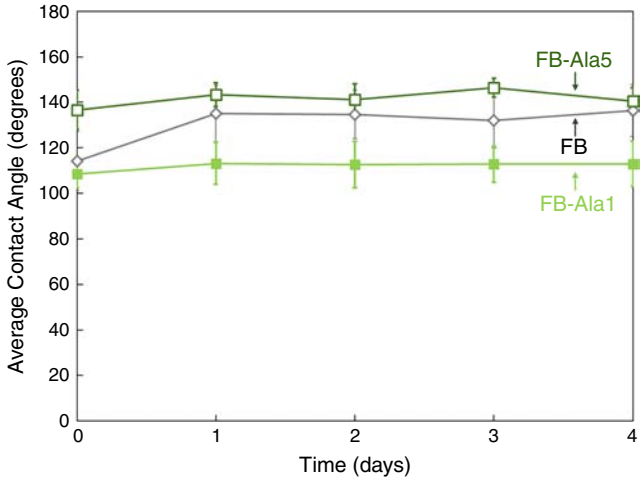

Fig. 12—Contact angle measurements for *β*-alanine in FB solutions at 368 K.

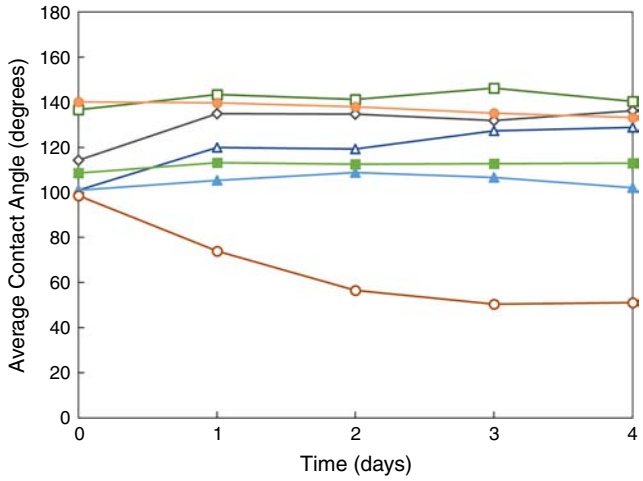

Fig. 13—Summary of contact angle results with brine solutions at 368 K.

Results in the current and previous subsections indicate that the presence of ionic components in the FB might have affected the absorption of glycine and *β*-alanine on calcite. The impact of salts appeared to be more significant for *β*-alanine because the *β*-alanine solutions in the FB did not result in a meaningful reduction in contact angle, unlike the *β*-alanine solutions in DI water in the previous subsection. Glycine's pI, 5.97, is clearly lower than the pH values of FB, IB1, and IB2, but *β*-alanine's pI, 6.89, is likely too high to make a clear change in the contact angle in the saline solutions tested. That is, glycine was overall in the anionic form in the solution, which was suitable for interaction with the positively charged calcite surface. *β*-alanine, however, did not have a sufficiently negative charge in the saline solutions tested.

It was clear that FB-Gly5 was superior to FB-Gly1 in altering the wettability of calcite surfaces toward a more water-wet state. This indicates that 1.0 wt% was below a minimum loading of glycine for a meaningful change in wettability in this experiment. There would be more probable collisions of glycine with the calcite surface at a higher concentration, leading to the wettability alteration toward a more water-wet state.

β-alanine was incapable of changing the wettability of oil-wet calcite surfaces to water-wet likely because of the electrostatic repulsions between the calcite surface and *β*-alanine molecules that are both positively charged overall. One interesting observation in the contact angle experiment with *β*-alanine is that FB-Ala1 has shown a contact angle that is approximately 15° lower than that of FB-Ala5. This can be because the positively charged *β*-alanine molecules contribute to the total salinity of the solution. Therefore, FB-Ala5 has increased the contact angle in comparison to FB-Ala1.

Spontaneous and Forced Imbibition Experiments. The imbibition experiments were focused on glycine because of the clear advantage of glycine over *β*-alanine in the contact angle experiment (Contact Angle Experiment #2 section). IB-2 was chosen as the base case with no glycine because many publications on low-salinity waterflooding indicate that IB-2 is expected to perform better than IB-1 and FB in oil recovery (Myint and Firoozabadi 2015; Bartels et al. 2019).

When the core plugs were immersed in the solutions, no oil recovery was observed. This indicated that the cores were oil-wet after aging at 368 K for 3 weeks. The experiment was concluded on Day 28 after no more oil recovery was observed for 10 days. **Fig. 14** shows the oil recovery factors obtained by spontaneous imbibition with four aqueous solutions: IB2, IB2 with 5 wt% glycine (IB2-Gly5), IB1 with 5 wt% glycine (IB1-Gly5), and FB with 5 wt% glycine (FB-Gly5). The final oil recovery from the spontaneous imbibition was 30.9% with FB-Gly5, 30.0% with IB1-Gly5, 21.7% with IB2-Gly5, and 11.3% with IB2.

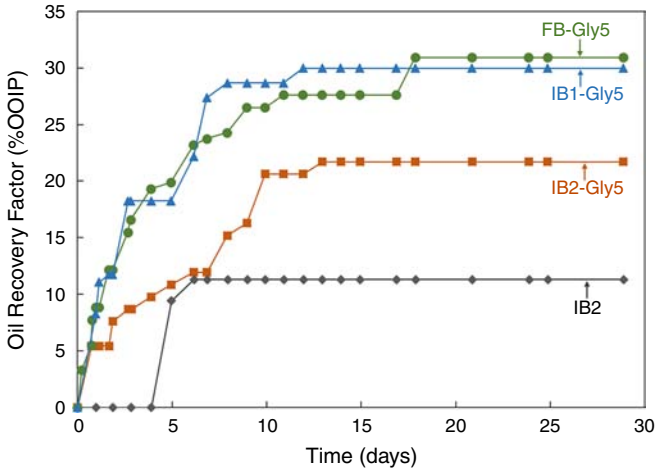

Fig. 14—Oil recovery factors for the spontaneous imbibition experiments at 368 K.

The oil recovery factors in Fig. 14 (particularly the IB2 case) are not smooth because oil droplets from the core surfaces were released discontinuously and because the oil droplets tended to be large for less water-wet cores (e.g., IB2) with the large viscosity of the oil used in this research. This type of oil recovery behavior was reported by other researchers using viscous oil (Meng et al. 2017). Mason and Morrow (2013) recommended either shaking the sample or gently brushing the core surface with a strongly oil-wet rod to force the detachment of oil droplets from the surfaces. However, we did not take any of these measures because doing so requires disturbing the experimental conditions, such as temperature.

The spontaneous imbibition was followed by forced imbibition for each core. **Fig. 15** shows the resulting oil recovery curves in terms of original oil in place (OOIP). **Fig. 16** shows the pressure drop measured during the experiment and the effluent's pH. The effluent pH is above glycine's pI, assuring the presence of the anionic form of glycine that interacts with positively charged carbonate surfaces. The ultimate oil volume recovered at the increased injection rate was used to calculate the Amott index to water for each case.

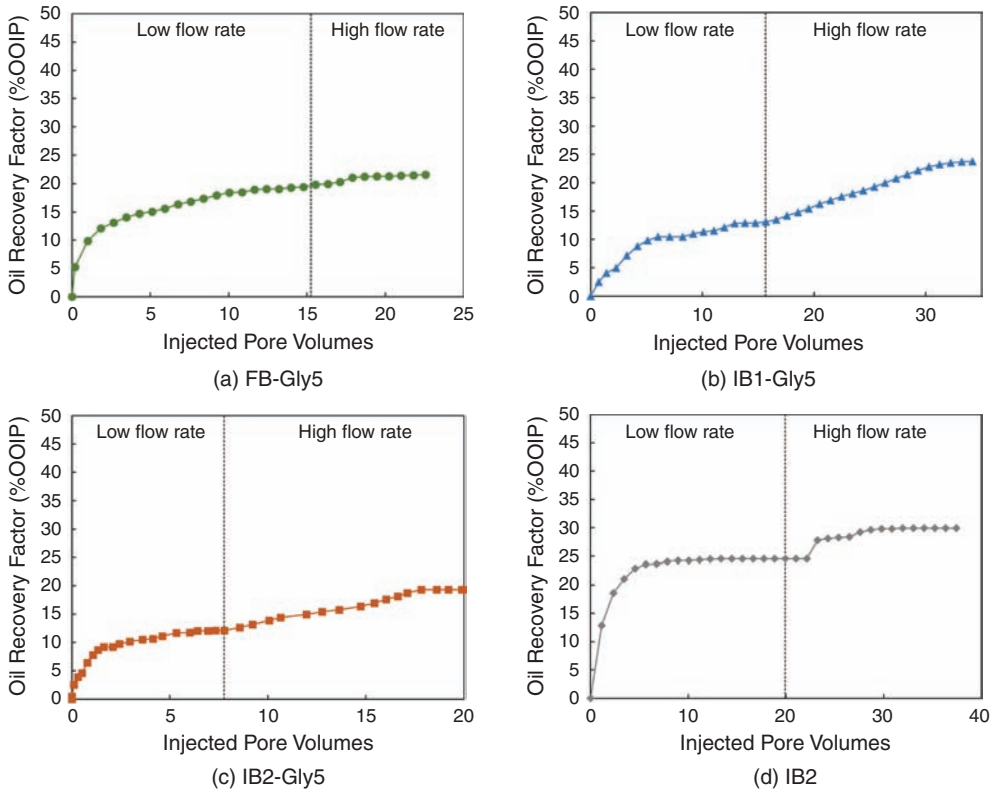

Fig. 15—Oil recovery curves from forced imbibition experiments in terms of the OOIP, i.e., the initial oil volume before the spontaneous imbibition. The increased oil recovery with the higher flow injection rate indicates the presence of the capillary end effect.

The results of the spontaneous and forced imbibition experiments are summarized in **Table 8.** After monitoring the oil recovery by spontaneous imbibition for 28 days, the Amott cells were moved to another oven before the forced imbibition experiments. During this time, there was an additional oil recovery, which was considered as part of spontaneous imbibition for the calculation of the Amott index to water. The resulting Amott index to water is 0.65 for FB-Gly5, 0.59 for IB1-Gly5, 0.61 for IB2-Gly5, and 0.33 for IB2. This clearly indicates that the solutions with glycine altered the rock wettability to more water state in comparison to IB2.

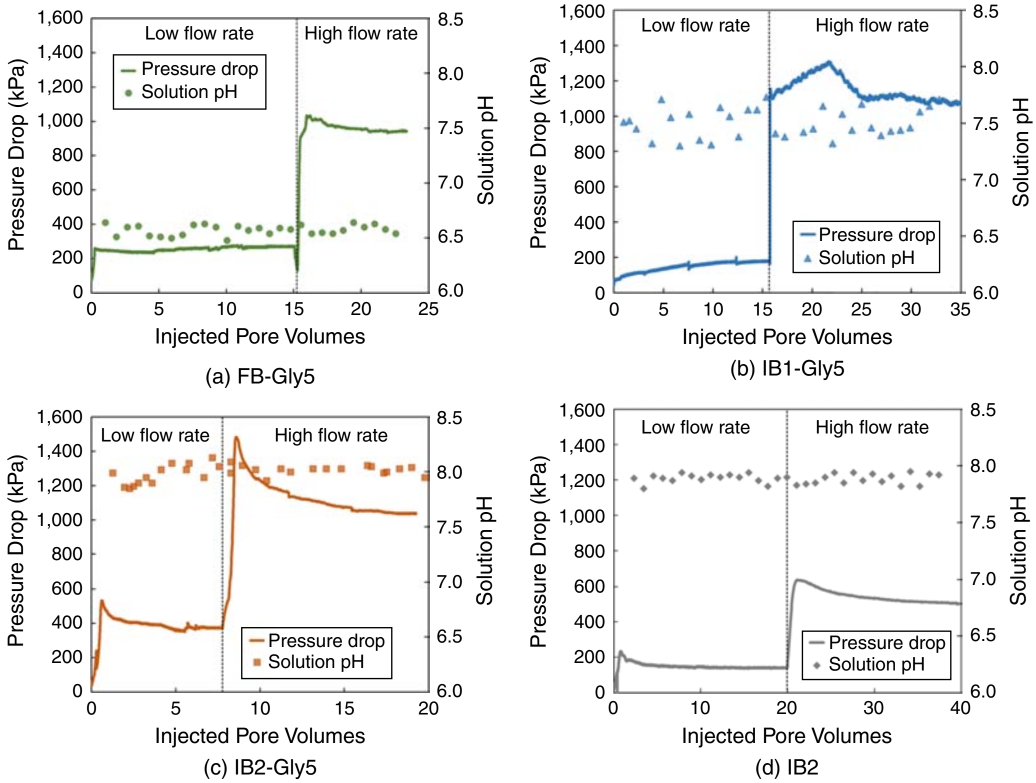

Fig. 16—Pressure drop and solution pH from forced imbibition experiments. The reported pH values were measured at room temperature.

Cumulative Oil Recovery (%OOIP)

Solution	Spontaneous Imbibition	Forced Imbibition: Low Injection Rate	Forced Imbibition: High Injection Rate	Amott Index to Water
FB-Gly5	30.9	49.4	52.5	0.65
IB1-Gly5	30.0	43.4	53.8	0.59
IB2-Gly5	21.7	33.8	41.1	0.61
IB2	11.3	35.9	41.3	0.33

Table 8—Cumulative oil recovery for spontaneous imbibition and forced imbibition experiments in terms of the original oil in place. The Amott index to water was calculated considering the ultimate oil volume recovered from forced imbibition experiments.

Although the core plugs were taken from the same block, the substantial heterogeneity in Indiana limestone should be taken into account for the interpretation of data from different core plugs. To decouple the impact of different petrophysical properties of the core plugs from the oil recovery performance, the oil recovery factors were plotted using the dimensionless time (t_d) given by Xie and Morrow (2001)

$$t_d = t\sqrt{\frac{k}{\phi}}\frac{\sigma}{\sqrt{\mu_o\mu_w}}\frac{4(d^2+L^2)}{L^2d^2}, \quad (8)$$

where k is the permeability, ϕ is the porosity, L is the core plug length, d is the core diameter, σ is the oil/brine IFT, and μ_o and μ_w are, respectively, the oleic and aqueous phase viscosity.

Moreover, the differences in initial water saturation and residual oil saturation among the cores were taken into account by expressing the oil recovery factor (RF) in terms of recoverable oil,

$$\mathrm{RF} = \frac{V_{o,\mathrm{produced}}}{V_{o,\mathrm{recoverable}}}, \quad (9)$$

where $V_{o,\mathrm{produced}}$ is the volume of oil produced. The volume of recoverable oil, $V_{o,\mathrm{recoverable}}$, is defined as

$$V_{o,\mathrm{recoverable}} = V_{\mathrm{pore}}(1 - S_{\mathrm{wi}} - S_{\mathrm{or}}), \quad (10)$$

where V_{pore} is the rock PV, S_{wi} is the initial water saturation, and S_{or} is the residual oil saturation after forced imbibition.

Note that the Amott index to water expressed in Eq. 1 is the RF calculated for the spontaneous imbibition using Eq. 9 because the recoverable oil from Eq. 10 is the denominator of Eq. 1. **Fig. 17** shows the resulting oil recovery plot with respect to the square root of

dimensionless time for the spontaneous imbibition experiments. Although the nonsmooth oil recovery curves make it unclear, the recovery curves generally follow a linear trend before leveling off. This indicates that the oil recovery process was dominated by the capillary driven countercurrent flow (Morrow and Mason 2001; Zhou et al. 2002). The comparison between the glycine solutions and IB2 in Fig. 17 clearly shows the positive impact of glycine on oil recovery by spontaneous imbibition. It is not clear from Fig. 17 how the brine composition and salinity affect the oil recovery mechanisms with glycine because the curves for FB-Gly5, IB1-Gly5, and IB2-Gly5 are close to one another.

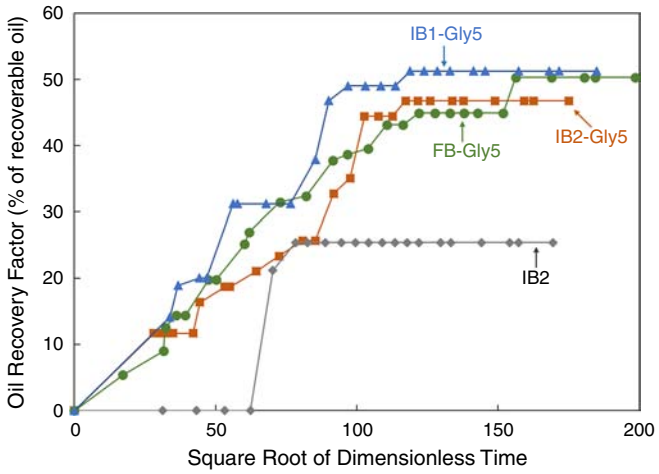

Fig. 17—Oil recovery factors in terms of the movable oil volume with respect to the squared-root of dimensionless time (Xie and Morrow 2001). The oil recovery factors show a linear relation typical of capillary-driven water imbibition.

The positive impact of glycine on oil recovery was reconfirmed by flooding the core for the IB2 case with IB2-Gly5 (i.e., tertiary flooding). The forced imbibition with IB2 was performed for a larger injected pore volume than the other cases to ensure that the core's residual oil to IB2 had been reached (Fig. 15d). **Fig. 18** shows the resulting recovery curve from the injection of IB2 followed by IB2-Gly5 at low and high injection rates. The results indicate that the injection of IB2-Gly5 yielded an additional oil recovery of 3.8% at the lower rate. Since the capillary number was reduced from the previous IB2 injection at a higher rate, the incremental oil recovery is attributed to the effect of glycine on wettability. The subsequent injection of IB2-Gly5 at a higher rate resulted in an additional recovery of 2.3%. The injection of IB2-Gly5 after IB2 resulted in a total incremental oil recovery of 6.1%. Note again that this experiment was to reconfirm the wettability alteration by glycine, instead of testing using glycine for tertiary flooding.

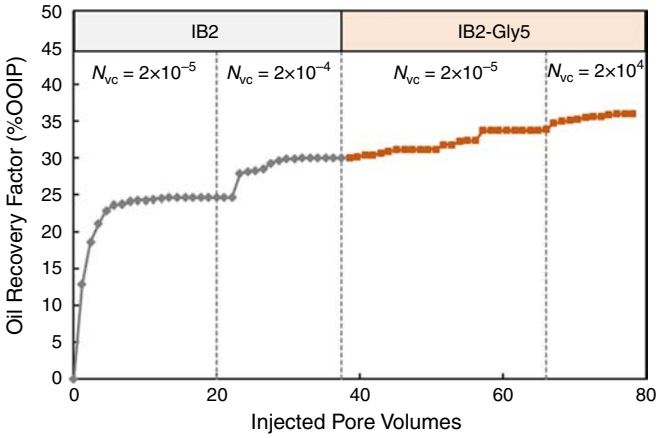

Fig. 18—Oil recovery curve for IB2 followed by the injection of IB2-Gly5. The addition of 5 wt% glycine to IB2 resulted in an incremental oil recovery of 6.1%. The increased oil recovery at a higher injection rate indicates the presence of the capillary end effect.

Discussion

The results presented above collectively indicate that the addition of glycine to the IB can increase oil recovery by wettability alteration in calcite-rich media. This wettability alteration requires the anionic form of glycine to interact with positively charged rock surfaces, causing the removal of polar oil components from the surfaces. The interaction of glycine with rock surfaces was confirmed by measuring the glycine concentration in the brine after the spontaneous imbibition experiments. Results showed the glycine adsorption of 0.23 mg/g-rock for the FB-Gly5 case, 0.27 mg/g-rock for the IB1-Gly5 case, and 0.24 mg/g-rock for the IB2-Gly5 case. These results are within and on the lower side of the surfactant retention measured for surfactant flooding of carbonate rocks, 0.21–1.9 mg/g-rock (Wang et al. 2019).

The solution pH should be above glycine's pI for glycine to interact with positively charged rock surfaces as discussed previously. Although common pI values for glycine have been reported in the literature, they were measured at room conditions in a diluted solution (Včeláková et al. 2004). Glycine's actual pI is likely different for different brines and at high temperatures (i.e., reservoir

temperature). Unfortunately, experimental data are scarce about the dependence of glycine's pI on temperature and the solution's ionic strength.

The model developed by De Stefano et al. (2000) is discussed to see the impact of brine composition and salinity on glycine's pI. This model considers glycine's speciation in seawater containing Na^+, K^+, Ca^{2+}, Mg^{2+}, Cl^-, and SO_4^{2-} ions. The protonation constants (pK_a) for the amino group and carboxyl group were estimated in relation to the ionic strength using the Debye-Hückel equation and Pitzer equations. These protonation constants can be used to calculate glycine's pI, since glycine's pI is the arithmetic average of the two pK_a values.

Fig. 19 (De Stefano et al. 2000) shows the comparison between glycine's speciation in pure water and in a brine with a salinity of 86,000 mg/L consisting of NaCl 0.25 mol/L and $MgCl_2$ 0.25 mol/L. It can be observed that the pK_a value of the amino group of glycine in the brine was shifted about one unit of pH in comparison to the pure water case. This indicates that glycine's pI decreased because of the combined effect of the increased ionic strength and the interactions between glycine and Na^+ and Mg^{2+} ions. A reduction in the pI causes the population of glycine's anionic form to increase, leading to more interaction of glycine with positively charged rock surfaces. Further investigation is required for a systematic understanding of the impact of glycine on oil recovery from carbonate rocks for different brine compositions and salinities.

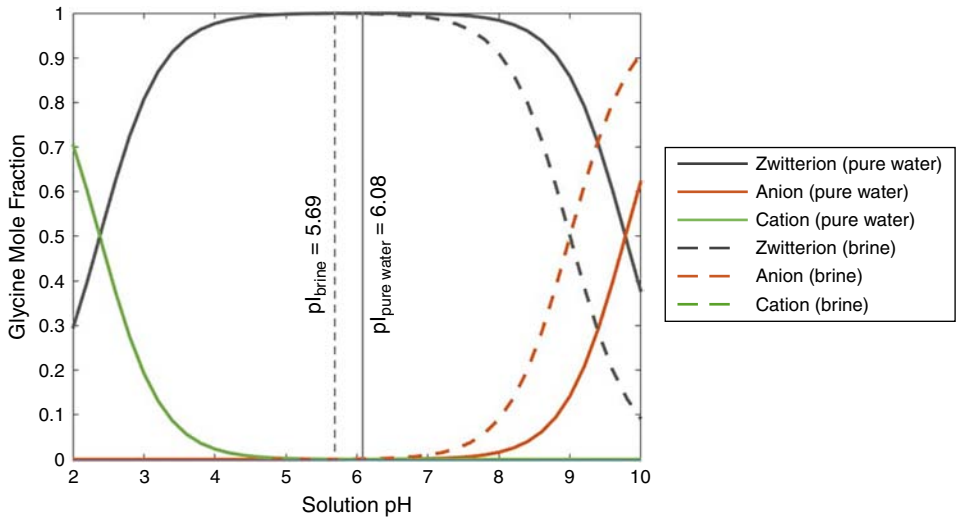

Fig. 19—Calculated distribution of glycine's species (zwitterion, anion, and cation) in DI water (continuous line) and brine (NaCl 0.25–$MgCl_2$ 0.25 mol/L) (dashed line). The brine has an ionic strength of 0.85 mol/L and a salinity of 86,000 mg/L. The pK_a value of the carboxyl group is the pH value at which the cation (green line) and the zwitterion (dark line) concentrations are equal. The pK_a value of the amino group is the pH value at which the anion (orange line) and the zwitterion (dark line) concentration are equal. The pI values were calculated reading the pK_a values of the plot in De Stefano et al. (2000). This figure is a modification of the original figure from therein.

The three glycine solutions (FB-Gly5, IB1-Gly5, and IB2-Gly5) resulted in similar oil recovery factors from the spontaneous imbibition as given in Fig. 17. The small differences among these glycine cases might be related to the solution pH. Glycine has a tendency to lower the solution pH as confirmed by a separate set of experiments with no calcite piece. In the imbibition experiment with glycine, the reduced pH might have lowered the zeta potential of the rock surfaces. This is consistent with the previous studies by Alotaibi et al. (2011) and Mahani et al. (2017), who showed a positive correlation between surface zeta potential and solution pH in their zeta potential experiments for limestone in seawater.

In summary, glycine likely has a direct and indirect impact on rock wettability. The direct impact is that glycine lowers the polar–polar interaction of oil components with positively charged rock surfaces when the solution pH is between the surface pzc and the glycine pI. Under these conditions, the interaction of the anionic form of glycine with the positively charged calcite surface releases oil which was anchored by carboxylate groups of the naphthenic acids. Furthermore, the indirect impact is that glycine slightly lowers the solution pH, which in turn lowers the zeta potential of rock surfaces. Although this indirect impact is considered to be a minor factor, it may also contribute to the wettability alteration for increasing oil recovery.

Further investigation is necessary for the potential application of amino acids for enhanced waterflooding. Next research tasks include fundamental investigation into the interaction of amino acids with rock surfaces and core floods at different conditions in terms of rock type, matrix/fracture configuration, flow regime, and amino acid injection strategy. Numerical reservoir simulation studies are also necessary for scaling up to potential field applications.

Conclusions

This paper presented an experimental investigation of amino acids as an additive to brine for improved waterflooding in carbonate reservoirs. The amino acids tested in this research are glycine and β-alanine. The contact angle experiments with polished calcite pieces demonstrated that glycine was superior to β-alanine as a wettability modifier in brine. Glycine was further tested in the imbibition experiments (spontaneous and forced) to confirm the increase in oil recovery by wettability alteration from oil-aged limestone cores. Conclusions are as follows:

- The contact angle experiment with DI water at room temperature (Contact Angle Experiment #1 section) confirmed that glycine can alter the wettability of oil-aged calcite from oil-wet to strongly water-wet when the solution pH is between the glycine pI (5.97) and the calcite pzc (8.8). The wettability alteration was also confirmed at pH values lower than the glycine pI, and this was attributed to calcite dissolution. The calcite dissolution at low pH values can be enhanced by the presence of glycine in the solution because glycine tends to suppress the pH increase by deprotonation of the carboxyl group.

- The pI values of glycine and β-alanine depend on temperature and brine composition. The contact angle experiments with brines at 368 K (Contact Angle Experiment #2 section) indicated that glycine was effective in lowering the contact angle in brines (pH values between 7.0–7.9) as long as a sufficient amount of glycine is available for the interaction with the oil-wet surface. β-alanine was not effective in wettability alteration of oil-aged calcite with the brines tested at 368 K.
- The imbibition experiment with Indiana limestone cores (Spontaneous and Forced Imbibition Experiments section) showed that glycine can enhance the oil recovery by spontaneous imbibition. The oil recovery factor by IB2 was 11.3%, but the addition of 5 wt% glycine in IB2 (IB2-Gly5) yielded the oil recovery factor of 21.7% by spontaneous imbibition. The impact of glycine on wettability alteration was also confirmed by the tertiary flooding by IB2-Gly5 after the IB2 flooding, which yielded 6.1% additional oil recovery.
- The recovery factor from spontaneous imbibition on the basis of the recoverable oil for each core was 81.3% for FB-Gly5, 76.4% for IB1-Gly5, 79.2% for IB2-Gly5, and 49.2% for IB2. The recovery factors resulted in the Amott index to water as follows: 0.65 for FB-Gly5, 0.59 for IB1-Gly5, 0.61 for IB2-Gly5, and 0.33 for IB2. This indicates clearly that the addition of glycine to brines can significantly change the rock's wettability toward a more water-wet state. The results also indicated that the effect of brine salinity and composition might be small on the wettability alteration by glycine.
- Analysis of experimental results indicated two possible mechanisms of glycine to enhance the spontaneous imbibition in oil-aged carbonate rocks. The main mechanism is that the glycine solution weakens the interaction between polar oil components and positively charged rock surfaces when the solution pH is between the glycine pI and the surface pzc. Another minor mechanism is that the addition of glycine tends to decrease the solution pH slightly, which in turn decreases the surface charge and changes the carbonate wettability in brines to a more water-wet state.
- Glycine was found to be quite stable with the brines tested in this research. Up to 10 wt% loading in FB, IB1, and IB2 did not show any precipitation at 298 K. Glycine is nontoxic, widely used in the food industry, and commercially available at relatively low cost.

Nomenclature

d = core plug diameter, m
L = core plug length, m
k = permeability, m^2
k_1 = calcite dissolution rate constant
K_a = acid dissociation constant
k°_{rw} = endpoint water relative permeability
pK_a = negative base-10 log of the acid dissociation constant
R = rate of calcite dissolution, mmol/cm^2·s
S_{or} = residual oil saturation, v/v
S_{wi} = initial water saturation, v/v
t = time, s
t_d = dimensionless time
u = superficial velocity, m/s
v = interstitial velocity, m/s
$V_{o,produced}$ = produced oil volume, cm^3
$V_{o,recoverable}$ = recoverable oil volume, cm^3
V_{pore} = PV, cm^3
θ = oil/water contact angle, degrees
μ_o = oil viscosity, Pa·s
μ_w = water viscosity, Pa·s
σ = water/oil IFT, N/m
ϕ = porosity, v/v

Acknowledgments

We gratefully acknowledge the financial support from Saudi Aramco. Ryosuke Okuno holds the Pioneer Corporation Faculty Fellowship in Petroleum Engineering at the University of Texas at Austin. Larry W. Lake holds the Shahid and Sharon Ullah Chair at the University of Texas at Austin.

References

Al Mahrouqi, D., Vinogradov, J., and Jackson, M. D. 2017. Zeta Potential of Artificial and Natural Calcite in Aqueous Solution. *Adv Colloid Interface Sci* **240:** 60–76. https://doi.org/10.1016/j.cis.2016.12.006.

Alotaibi, M. B. and Yousef, A. A. 2017. The Role of Individual and Combined Ions in Waterflooding Carbonate Reservoirs: Electrokinetic Study. *SPE Res Eval & Eng* **20** (1): 77–86. SPE-177983-PA. https://doi.org/10.2118/177983-PA.

Ayirala, S. C., Saleh, M. E., Enezi, S. M. et al. 2018. Effect of Salinity and Water Ions on Electrokinetic Interactions in Carbonate Reservoirs Cores at Elevated Temperatures. *SPE Res Eval & Eng* **21** (3): 733–746. SPE-189444-PA. https://doi.org/10.2118/189444-PA.

Bartels, W. B., Mahani, H., Berg, S. et al. 2019. Literature Review of Low Salinity Waterflooding from a Length and Time Scale Perspective. *Fuel* **236:** 338–353. https://doi.org/10.1016/j.fuel.2018.09.018.

Brantley, S. L., Kubicki, J. D., and White, A. F. 2007. *Kinetics of Water-Rock Interaction*, first edition. New York, New York, USA: Springer Science & Business Media.

Buckley, J. S., Takamura, K., and Morrow, N. R. 1989. Influence of Electrical Surface Charges on the Wetting Properties of Crude Oils. *SPE Res Eng* **4** (3): 332–340. SPE-16964-PA. https://doi.org/10.2118/16964-PA.

Chen, S., Kristiansen, K., Seo, D. et al. 2018. Time-Dependent Physicochemical Changes of Carbonate Surfaces from SmartWater (Diluted Seawater) Flooding Processes for Improved Oil Recovery. *Langmuir* **35** (1): 41–50. https://doi.org/10.1021/acs.langmuir.8b02711.

Churcher, P. L., French, P. R., and Shaw, J. C. 1991. Rock Properties of Berea Sandstone, Baker Dolomite, and Indiana Limestone. Paper presented at the SPE International Symposium on Oilfield Chemistry, Anaheim, California, USA, 20–22 February. SPE-21044-MS. https://doi.org/10.2118/21044-MS.

Churchill, H., Teng, H., and Hazen, R. M. 2004. Correlation of pH-Dependent Surface Interaction Forces to Amino Acid Adsorption: Implications for the Origin of Life. *Am Mineral* **89** (7): 1048–1055. https://doi.org/10.2138/am-2004-0716.

De Stefano, C., Foti, C., Gianguzza, A. et al. 2000. The Interaction of Amino Acids with the Major Constituents of Natural Waters at Different Ionic Strengths. *Mar Chem* **72** (1): 61–76. https://doi.org/10.1016/S0304-4203(00)00067-0.

Ghosh, P., Sharma, H., and Mohanty, K. K. 2018. Development of Surfactant-Polymer SP Processes for High Temperature and High Salinity Carbonate Reservoirs. Paper presented at the SPE Annual Technical Conference and Exhibition, Dallas, Texas, USA, 24–26 September. SPE-191733-MS. https://doi.org/10.2118/191733-MS.

Heberling, F., Trainor, T. P., Lützenkirchen, J. et al. 2011. Structure and Reactivity of the Calcite–Water Interface. *J Colloid Interface Sci* **354** (2): 843–857. https://doi.org/10.1016/j.jcis.2010.10.047.

Hiorth, A., Cathles, L. M., and Madland, M. V. 2010. The Impact of Pore Water Chemistry on Carbonate Surface Charge and Oil Wettability. *Transp Porous Media* **85** (1): 1–21. https://doi.org/10.1007/s11242-010-9543-6.

Hirasaki, G. J. 1991. Wettability: Fundamentals and Surface Forces. *SPE Form Eval* **6** (2): 217–226. SPE-17367-PA. https://doi.org/10.2118/17367-PA.

Høgnesen, E. J., Strand, S., and Austad, T. 2005. Waterflooding of Preferential Oil-Wet Carbonates: Oil Recovery Related to Reservoir Temperature and Brine Composition. Paper presented at the SPE Europec/EAGE Annual Conference, Madrid, Spain, 13–16 June. SPE-94166-MS. https://doi.org/10.2118/94166-MS.

Karty, K. 2018. *Organic Chemistry: Principles and Mechanisms*, second edition. New York, New York, USA: W.W. Norton & Company.

Lake, L. W., Johns, R., Rossen, W. R. et al. 2014. *Fundamentals of Enhanced Oil Recovery*, second edition. Richardson, Texas, USA: Society of Petroleum Engineers.

Langmuir, D. 1997. *Aqueous Environmental Geochemistry*, first edition. Upper Saddle River, New Jersey, USA: Prentice Hall.

Madani, M., Zargar, G., Takassi, M. A. et al. 2019. Fundamental Investigation of an Environmentally-Friendly Surfactant Agent for Chemical Enhanced Oil Recovery. *Fuel* **238** (15): 186–197. https://doi.org/10.1016/j.fuel.2018.10.105.

Mahani, H., Keya, A. L., Berg, S. et al. 2017. Electrokinetics of Carbonate/Brine Interface in Low-Salinity Waterflooding: Effect of Brine Salinity, Composition, Rock Type, and pH on ζ-Potential and a Surface-Complexation Model. *SPE J.* **22** (1): 53–68. SPE-181745-PA. https://doi.org/10.2118/181745-PA.

Mason, G. and Morrow, N. R. 2013. Developments in Spontaneous Imbibition and Possibilities for Future Work. *J Pet Sci Eng* **110:** 268–293. https://doi.org/10.1016/j.petrol.2013.08.018.

Meng, Q., Liu, H., and Wang, J. 2017. A Critical Review on Fundamental Mechanisms of Spontaneous Imbibition and the Impact of Boundary Condition, Fluid Viscosity and Wettability. *Adv Geo-Energy Res* **1** (1): 1–17. https://doi.org/10.26804/ager.2017.01.01.

Morrow, N. R. and Mason, G. 2001. Recovery of Oil by Spontaneous Imbibition. *Curr Opin Colloid Interface Sci* **6** (4): 321–337. https://doi.org/10.1016/S1359-0294(01)00100-5.

Myint, P. C. and Firoozabadi, A. 2015. Thin Liquid Films in Improved Oil Recovery from Low-Salinity Brine. *Curr Opin Colloid Interface Sci* **20** (2): 105–114. https://doi.org/10.1016/j.cocis.2015.03.002.

Plummer, L. N., Wigley, T. M. L., and Parkhurst, D. L. 1978. The Kinetics of Calcite Dissolution in CO_2-Water Systems at 5° to 60°C and 0.0 to 1.0 atm CO_2. *Am J Sci* **278** (2): 179–216. https://doi.org/10.2475/ajs.278.2.179.

Rapoport, L. A. and Leas, W. J. 1953. Properties of Linear Waterfloods. *J Pet Technol* **5** (5): 139–148. SPE-213-G. https://doi.org/10.2118/213-G.

Sjöberg, E. L. and Rickard, D. T. 1984. Temperature Dependence of Calcite Dissolution Kinetics between 1 and 62°C at pH 2.7 to 8.4 in Aqueous Solutions. *Geochim Cosmochim Acta* **48** (3): 485–493. https://doi.org/10.1016/0016-7037(84)90276-X.

Strand, S., Høgnesen, E. J., and Austad, T. 2006. Wettability Alteration of Carbonates—Effects of Potential Determining Ions (Ca^{2+} and SO_4^{2-}) and Temperature. *Colloids Surf A Physicochem Eng Asp* **75** (1–3): 1–10. https://doi.org/10.1016/j.colsurfa.2005.10.061.

Tagavifar, M., Sharma, H., Wang, D. et al. 2018. Alkaline/Surfactant/Polymer Flooding with Sodium Hydroxide in Indiana Limestone: Analysis of Water/Rock Interactions and Surfactant Adsorption. *SPE J.* **23** (6): 2279–2301. SPE-191146-PA. https://doi.org/10.2118/191146-PA.

Tripathy, D. B., Mishra, A., Clark, J. et al. 2018. Synthesis, Chemistry, Physicochemical Properties and Industrial Applications of Amino Acid Surfactants: A Review. *C R Chim* **21** (2): 112–130. https://doi.org/10.1016/j.crci.2017.11.005.

Včeláková, K., Zusková, I., Kenndler, E. et al. 2004. Determination of Cationic Mobilities and pKa values of 22 Amino Acids by Capillary Zone Electrophoresis. *Electrophoresis* **25** (2): 309–317. https://doi.org/10.1002/elps.200305751.

Wang, D., Maubert, M., Pope, G. A. et al. 2019. Reduction of Surfactant Retention in Limestones Using Sodium Hydroxide. *SPE J.* **24** (1): 92–115. SPE-194009-PA. https://doi.org/10.2118/194009-PA.

Xie, X. and Morrow, N. R. 2001. Oil Recovery by Spontaneous Imbibition from Weakly Water-Wet Rocks. *Petrophysics* **42** (4): SPWLA-2001-v42n4a1.

Yousef, A. A., Al-Saleh, S. H., Al-Kaabi, A. et al. 2011. Laboratory Investigation of the Impact of Injection-Water Salinity and Ionic Content on Oil Recovery from Carbonate Reservoirs. *SPE Res Eval & Eng* **14** (5): 578–593. SPE-137634-PA. https://doi.org/10.2118/137634-PA.

Zhang, P., Tweheyo, M. T., and Austad, T. 2007. Wettability Alteration and Improved Oil Recovery by Spontaneous Imbibition of Seawater into Chalk: Impact of the Potential Determining Ions Ca^{2+}, Mg^{2+}, and SO_4^{2-}. *Colloids Surf A Physicochem Eng Asp* **301** (1–3): 199–208. https://doi.org/10.1016/j.colsurfa.2006.12.058.

Zhou, D., Jia, L., Kamath, J. et al. 2002. Scaling of Counter-Current Imbibition Processes in Low-Permeability Porous Media. *J Pet Sci Eng* **33** (1–3): 61–74. https://doi.org/10.1016/S0920-4105(01)00176-0.

Ricardo A. Lara Orozco is a PhD-degree candidate in petroleum engineering at the University of Texas at Austin. His current research interests include reservoir engineering and EOR. Lara Orozco holds a bachelor's degree in chemical engineering from Instituto Tecnológico de Villahermosa and a master's degree from Instituto Mexicano del Petróleo. He is a member of SPE.

Gayan A. Abeykoon is a postdoctoral fellow in the Department of Petroleum and Geosystem Engineering at the University of Texas at Austin. His current research interests include phase behavior, novel additives for tight oil and heavy-oil recovery, and development of surfactant formulations for EOR. Abeykoon holds a PhD degree in organic chemistry from Iowa State University. He is a member of SPE.

Mingyuan Wang is a PhD-degree candidate in petroleum engineering in the Hildebrand Department of Petroleum and Geosystems Engineering at the University of Texas at Austin. His current research interests include phase behavior, EOR, and unconventional resources. Wang holds a bachelor's degree from the China University of Petroleum (Beijing) and a master's degree from the University of Alberta, both in petroleum engineering.

Francisco Javier Argüelles-Vivas is a postdoctoral fellow in the Hildebrand Department of Petroleum and Geosystems Engineering at the University of Texas at Austin. His current research interests are enhanced-oil-recovery methods for conventional/unconventional reservoirs, formation damage, phase behavior of bitumen/heavy-oil/solvent mixtures, pore-scale modeling, and carbon dioxide sequestration. Argüelles-Vivas holds a bachelor's degree in chemical engineering from the Metropolitan Autonomous University, Mexico; a master's degree in petroleum engineering from the Mexican Petroleum Institute; and a PhD degree in petroleum engineering from the University of Alberta. He is a member of SPE.

Ryosuke Okuno is an associate professor in the Hildebrand Department of Petroleum and Geosystems Engineering at the University of Texas at Austin. His research and teaching interests include EOR, thermal oil recovery, unconventional oil and gas, numerical reservoir simulation, thermodynamics, multiphase behavior, and applied mathematics. Okuno holds bachelor's and master's degrees in geosystem engineering from the University of Tokyo, and a PhD degree in petroleum engineering from the University of Texas at Austin.

Larry W. Lake is a professor and holder of the Shahid and Sharon Ullah at the University of Texas at Austin. His research is in EOR, geochemical modeling, reservoir characterization, and reservoir engineering. Lake is an SPE member.

Subhash C. Ayirala is a petroleum engineering specialist with 15 years of reservoir engineering experience in the oil industry. He currently leads the smart waterflooding focus area at Saudi Aramco's Exploration and Petroleum Engineering Center–Advanced Research Center, Dhahran, Saudi Arabia. Ayirala's research interests are in improved/EOR including advanced waterflooding, chemical EOR, and miscible CO_2 gas injection. He holds MS and PhD degrees in petroleum engineering from Louisiana State University, Baton Rouge. Ayirala is an SPE member.

Abdulkareem M. AlSofi is a reservoir engineer at Saudi Aramco's EXPEC ARC, where he is the champion of the chemical-enhanced-oil-recovery and heavy-oil-mobilization focus areas. He holds a BSc degree from the University of Texas at Austin and a PhD degree from Imperial College London, both in petroleum engineering.